Multinuclear NMR analysis of SAPO-34 gels in the presence and absence of HF: The initial gel

ARTICLE *in* THE JOURNAL OF PHYSICAL CHEMISTRY A · MARCH 1999

Impact Factor: 2.69 · DOI: 10.1021/jp983024p

Multinuclear NMR Analysis of SAPO-34 Gels in the Presence and Absence of HF: The Initial Gel

Ø. B. Vistad,*,†,‡ E. W. Hansen,† D. E. Akporiaye,† and K. P. Lillerud‡

SINTEF Applied Chemistry, P.O. Box 124, Blindern, 0314 Oslo, Norway, and Department of Chemistry, University of Oslo, P.O. Box 1033, Blindern, 0315 Oslo, Norway

Received: July 15, 1998; In Final Form: November 16, 1998

Gels prepared for the synthesis of SAPO-34, with morpholine as a structure-directing agent, have been characterized by multinuclear (^{1}H, ^{13}C, ^{19}F, ^{27}Al, and ^{31}P), high-resolution NMR at room temperature. Less complex solutions are prepared and analyzed to aid in the peak assignment. Although some spectral features remain unresolved, the overall analysis is qualitatively consistent with the expected complex chemistry taking place in these solutions. Systems in the presence and absence of HF reveal significant spectral differences. It has been shown that pH can be monitored by the proton and carbon chemical shift of morpholine. In addition, ^{1}H and ^{13}C NMR spectra suggest that the structure-directing agent is an inactive species at room temperature independent of the presence or absence of HF. This is contrary to the ^{27}Al NMR, where it has been concluded that morpholine has a significant influence on the aluminum coordination, giving tetrahedral Al when HF is absent. The existence of octahedral aluminophosphate−fluoride complexes is evident in the presence of HF, while several octahedral aluminophosphate complexes are formed in the absence of HF and morpholine. No sign of interactions between aluminum and silicon, silicon and phosphates, silicon and morpholine, phosphates and morpholine, or morpholine and fluoride has been observed within the concentration range studied. Some time-resolved studies have revealed that the aging is shown to influence the type and the amount of species present in the solutions.

Introduction

Microporous solids, such as $AlPO_4$- and SAPO-type materials, are usually obtained by hydrothermal crystallization using various structure-directing agents (alkylammonium cations or organic amines). These materials were first reported by the workers at Union Carbide in the beginning of the 1980s.[1,2] Understanding the chemistry occurring in the aluminophosphate/silicoaluminophosphate solutions may contribute to the understanding of the processes involved in the nucleation and growth of the crystalline products. To achieve this, an experimental in situ technique is needed. NMR has shown promise for this purpose,[3] and this preliminary paper is devoted to the analysis of room-temperature phenomena occurring before the hydrothermal treatment. In addition, in situ synchrotron XRD has been shown fruitful for this purpose.[4] Furthermore, the effect of adding HF to the synthesis gel is one of the major subjects for this study.

In this work, attention has been given to the formation of SAPO-34. Several structure-directing agents are reported to be useful, and these include tetraethylammonium hydoxide,[2] morpholine,[5] piperidine,[6,7] diethylamine,[8] triethylamine,[9] and diisopropylamine.[2,10] This small-pore, chabazite-structure material has been shown to be an important methanol-to-olefin (MTO) catalyst.[11−13]

The synthesis procedure was optimized, both in the presence and absence of hydrofluoric acid. Consequently, under the same conditions and with the same recipe, the same product was obtained (after calcination), independent of the presence of HF. Therefore, it might be possible to obtain information about the role of the fluoride ions under the synthesis course, without altering any parameters other than the fluoride concentration.

NMR studies presented in the literature to date have been mainly restricted to simplified liquid solutions containing (1) a limited number of reactants (two- or three-component systems), (2) a pH range in which no solids or gels are formed, or (3) solutions of low ionic strength. Some of these papers are listed in Table 1. However, considering the synthesis conditions normally found when preparing AlPO's and SAPO's, the above outlined restrictions are normally not met. Of special importance, these solutions contain more than three reactants. With this in mind, the intention was to characterize, by multinuclear, high-resolution NMR, real synthesis solutions with relatively high ionic strengths and within pH ranges where both solids and gels coexist. In particular, these solutions will contain all species necessary to form the actual crystalline products.

It has been shown that the addition of polyphosphate ligands to Al^{3+} follows an "additivity law", with the ^{27}Al NMR chemical shift being proportional to the number of polyphosphate ligands bonded to the metal ion.[28,29] Principal changes in the ^{31}P NMR chemical shift are shown to be due to the nature of the ligands (H_3PO_4, $H_2PO_4^-$, HPO_4^{2-}, etc.), rather than the number of ligands in the complex.[23,25] These nuclei therefore give comparative information.

Prasad et al. have in their examination of $AlPO_4$ gels with ^{27}Al and ^{31}P NMR, proposed that framework units only are formed in the gels after addition of the structure-directing agent.[30−32] This is contrary to the investigations performed by He and Klinowski,[33] who proposed generation of framework Al before addition of the template. Furthermore, Marcuccilli-

* To whom correspondence should be addressed.
† SINTEF Applied Chemistry.
‡ University of Oslo.

10.1021/jp983024p CCC: $18.00
Published on Web 03/24/1999

TABLE 1: Overview of Previous Published NMR Data on Two- and/or Three-Component Systems

system	nucleus	ref
aluminosilicates prepared from SiO_2-Al-wire/HCl−KOH	^{27}Al, ^{29}Si	14
aluminosilicate species prepared from $SiO_2-Al(s)-NaOH$	^{27}Al, ^{29}Si	15
influence of silicate ratio and alkali metal cation size on aluminosilicate formation ($SiO_{2,(sol)}-Al(NO_3)_3-NaOH$)	^{27}Al, ^{29}Si	16
$Al(NO_3)_3-HF$	^{19}F and ^{27}Al	17
$AlCl_3 \cdot 6H_2O-KF$	^{19}F and ^{27}Al	18
$Al(NO_3)_3-NaF$ Vs pH	^{19}F and ^{27}Al	19
$AlCl_3/Al(NO_3)_3-HF/NH_4F$ and $Si(OH)_4-HF$	^{19}F, ^{27}Al, and ^{29}Si	20
$HF-H_2O-P_2O_5$	^{19}F and ^{31}P	21
$Al(NO_3)_3-H_3PO_4$	^{27}Al	22
$AlCl_3-H_3PO_4$ and $AlCl_3-H_3PO_4-NH_4F$	^{19}F, ^{27}Al, and ^{31}P	23
$AlCl_3/Al(NO_3)_3-Na_3PO_4-HCl/HNO_3$	^{31}P and ^{27}Al	24
$AlCl_3-H_{3-x}Na_xPO_4$	^{31}P and ^{27}Al	25
$AlCl_3/Al(NO_3)_3-H_3PO_4-TMA^a$	^{31}P and ^{27}Al	26
$AlCl_3/Al(NO_3)_3-H_3PO_4-TMA^a$ vs pH	^{31}P and ^{27}Al	27
$Al(NO_3)_3-$polyphosphates (this gave multivalent Al with cyclic phosphate, cP_n, ($P_nO_{3n}^{n-}$, $n = 3$, 4, 6, and 8) and long-chain polyphosphate anions	^{27}Al	28, 29

[a] Tetramethylammonium (TMA) hydroxide.

Hoffner has presented some multinuclear NMR investigation of some $AlPO_4$ gels, including gels with morpholine.[34]

In situ NMR studies of SAPO syntheses have not been reported. However, recently, Haouas et al.[3] reported multinuclear NMR investigation of the hydrothermal synthesis of $AlPO_4$−JC2 at temperatures up to 150 °C. In addition, Shi et al.[35] have performed in situ MAS NMR investigations on the crystallization of zeolite A at temperatures up to about 75 °C, giving zeolitic products after temperature treatment.

The aim of the present work is to use multinuclear, high-resolution NMR to obtain more insight into the complex chemistry within the gel phase before crystallization is initialized. Using the available NMR literature data, it was difficult to perform a proper peak assignment of the spectra. To help resolve these problems, NMR spectra of less complex solutions composed of all possible combinations of reactants (HF, Al_2O_3, SiO_2, P_2O_5, and morpholine) were made. The results will be discussed in the context of acidity (solutions pH), solution composition, dynamic exchange processes, and component solubility.

Experimental Section

Chemicals and Mixing Procedures. SAPO-34 was prepared in the presence and absence of HF. The final gel composition (mole ratio) used was 2.1 morpholine:1.0 SiO_2:1.0 Al_2O_3:1.0 P_2O_5:60 H_2O. Synthesis time and temperature were respectively 48 h and 200 °C. For the system containing fluoride, one equivalent HF was added resulting in faster nucleation and crystal growth. This resulted in a reduction in the synthesis time, which could be terminated after only 4−6 h.

The mixtures were prepared by first mixing one-fourth of the deionized water and 85 wt % phosphoric acid (Merck) together with the aluminum source (Catapal-B, Vista Chemicals). The mixture was then stirred well before further addition of one-fourth of deionized water. This mixture was labeled solution A. Solution B was prepared by mixing Ludox LS-30 (Du Pont), morpholine (Jansen Chemica), and yet another fourth of the water. This solution was then slowly added to solution A during intense mixing, before the last fourth of the water was added. Subsequently, 1 equiv of 40 wt % HF (Fluka) was added at the end of the preparation (applies to mixture 1−16). Since the reactant stoichiometry has been kept constant throughout the work, increased concentrations are archived when some or more of the reactants are omitted.

In addition to water, there are a maximum of five components in the final gel, resulting in 32 combinatorial different mixtures, as illustrated in Table 2. To keep track of the different mixtures and to make it easy to refer to a mixture with a specified composition, a letter code is introduced. This code is composed of one letter for each ingredient (F for hydrofluoric acid, A for pseudoboehmite (Al), S for Ludox (Si), P for phosphoric acid, and M for morpholine). Water is omitted from the code because all the mixtures are prepared in aqueous solutions.

The NMR analyses have been carried out at room temperature within only 15−30 min after preparation of the samples. The main reason for this short time delay between preparation of the mixtures and data sampling is because aging is not considered under ordinary synthesis conditions. It should be emphasized that equilibrium may not have been reached in all the mixtures, especially those containing aluminum. Earlier studies on similar aluminum-containing systems have shown that this may take years.

Characterization. Powder X-ray diffraction (XRD) patterns were collected on a Siemens D5000 diffractometer. The instrument was equipped with a Ge fully focusing primary monochromator ($Cu_{K\alpha 1}$ radiation, $\lambda = 1.540560$ Å) and a Brown 16° position-sensitive flat PSD detector. The step size used was 0.0154° (step time 1.0 s), and the scan range was 2−40° (2θ).

The pH measurements were performed with a Copenhagen Radiometer PHM82 standard pH meter.

The NMR measurements were performed at room temperature (25 °C) using a Varian VXR spectrometer operating at 7.05 T. The solution was confined in a 5 mm o.d. tube that was inserted into a 10 mm o.d. tube. The resulting free space between the two tubes was filled with D_2O, which was used as a lock solvent. To acquire quantitative NMR signal intensities, the repetition time was chosen to be about 5 times the longest spin−lattice relaxation time (T_1) for each of the nuclei investigated (^1H, ^{13}C, ^{19}F, ^{27}Al, ^{31}P). Regarding the ^{27}Al NMR experiments, a shortest possible pulse angle (corresponding to a rf pulse of 0.5 μs) was used in order to minimize the effect of signal decay during the pulse. This precaution was found necessary due to the short relaxation time of the quadrupolar nucleus. Signal intensity (area) was determined by numerical integration of the resonance peak or by curve fitting when severe overlap of peaks was observed. Of particular importance, both ^{19}F and ^{27}Al NMR revealed broad background signals originating from the probe design. To avoid interference from this unwanted signal in the quantitative analysis, the first few points in the NMR free

TABLE 2: Composition of the Different Mixtures and the Respective Letter Code

	H_2O	HF	Al_2O_3	SiO_2	P_2O_5	morpholine	pH	consistence	code
1	X	X					1.7	clear solution	F
2	X	X	X				4.2	white suspension	FA
3	X	X		X			2.0	clear solution, opalescent day after	FS
4	X	X			X		1.6	clear solution	FP
5	X	X				X	9.2	clear solution	FM
6	X	X	X	X			3.9	white geleous suspension	FAS
7	X	X	X		X		1.8	opalescent gel, high viscosity	FAP
8	X	X	X			X	9.5	bright-yellow gel, high viscosity	FAM
9	X	X		X	X		1.5	clear solution, opalescent day after	FSP
10	X	X		X		X	9.3	clear solution	FSM
11	X	X			X	X	3.5	clear solution	FPM
12	X	X	X	X	X		1.7	opalescent gel, high viscosity	FASP
13	X	X	X	X		X	9.3	bright-yellow gel, high viscosity	FASM
14	X	X	X		X	X	4.8	equal to 12, but higher viscosity	FAPM
15	X	X		X	X	X	2.9	clear solution	FSPM
16	X	X	X	X	X	X	5.6	opalescent gel, high viscosity	FASPM
17[a]	X								
18[b]	X		X						A
19	X			X			9.5	clear solution	S
20	X				X		1.6	clear solution	P
21	X					X	11.8	clear solution	M
22	X		X	X			7.0	white suspension	AS
23	X		X		X		2.4	opalescent gel, high viscosity	AP
24	X		X			X	11.6	white suspension	AM
25	X			X	X		1.8	clear solution	SP
26	X			X		X	11.6	clear solution	SM
27	X				X	X	5.0	clear solution	PM
28	X		X	X	X		2.1	opalescent gel, high viscosity	ASP
29[b]	X		X	X		X			ASM
30	X		X		X	X	5.7	opalescent gel, low viscosity	APM
31	X			X	X	X	4.4	clear solution	SPM
32	X		X	X	X	X	5.8	'milky solution', low viscosity	ASPM

[a] Contain only water and is therefore not examined. [b] Not examined because of insufficient dissolution of the aluminum source in these mixtures.

induction decay (FID) were deleted, and a linear (back) prediction algorithm was applied.[36] This approach was possible since all resonance peaks revealed Lorenzian line shape profiles.[37] All chemical shift measurements have been referenced to external liquid solutions containing TMS (^{1}H and ^{13}C), $Al(NO_3)_3$ (^{27}Al), $CFCl_3$ (^{19}F), and 85 wt % H_3PO_4 (^{31}P). These solutions are also applied to calculate the expected signal intensities ($I_{expected}$) and determine the amount of observed signal intensity ($I_{observed}$). Since the main intention of this work is to establish an in situ technique to follow the nucleation and crystallization, ^{29}Si NMR has not been applied. This is due the short synthesis time and the low sensitivity combined with long acquisition time for this nucleus.

Results and Discussion

The receipt for synthesis of SAPO-34 was optimized with morpholine as a structure-directing agent. Without HF in the gel, a pure trigonal SAPO-34 was obtained while a mixture of triclinic and trigonal SAPO-34 was obtained with HF. After calcination of the latter mixture at 580 °C in air, pure trigonal SAPO-34 was obtained. Typical X-ray patterns of the synthesized and calcined samples are given in Figure 1.

Morpholine Interactions Observed by ^{1}H and ^{13}C NMR. The main detectable signal in the ^{1}H NMR spectrum is the intense peak from bulk water in exchange with proton-containing acids (HF, $H_{3-x}PO_4^{-x}$), proton-containing complexes ($[Al(H_2O)_{6-x}F_x]^{+3-x}$, $[Al(H_{3-x}PO_4)_n]^{+3-nx}$, etc.), and morpholine. Any intermediate exchange rate, on the NMR time scale, between these proton-containing species and bulk water will result in line broadening and chemical shift variation, as discussed in previous studies.[38] Due to these dynamic exchange processes, it may be difficult, if not impossible, to obtain reliable and quantitative information regarding the water−metal ion complexes from ^{1}H NMR alone. However, the well-resolved peaks originating from morpholine (3.80 and 3.15 ppm) enables this species to be followed quantitatively and in situ during the synthesis reaction.

Recent room-temperature NMR studies[38] have suggested morpholine to be an inert species at least in the less complex mixtures. This is rather fortunate, because it enables the pH of the gel solution to be estimated from the ^{13}C NMR chemical shift of morpholine, as illustrated in Figure 2. Also, the ^{1}H NMR chemical shift of morpholine can be used. If the ^{13}C NMR chemical shift at any stage during a synthesis reaction falls outside the region depicted in Figure 2, it will indicate that morpholine interacts with other species in solution and thus becomes an active species itself.

No interaction between morpholine and fluorides, phosphates, or silicates has been observed in this work.

Fluoride Interactions Observed by ^{19}F NMR. The majority of the ^{19}F NMR resonance peaks from the less complex mixtures can be assigned from the literature (Table 3) and are summarized in Table 4. The spectra are shown in Figure 3.

Mixture F contains only diluted HF. The observed single resonance peak at $\delta = -158.73$ ppm (Figure 4,F) is in agreement with the rapid exchange of F between the HF, F^-, and HF_2^- species.[38]

The ^{19}F NMR spectrum of the FA mixture gives evidence of interaction between aluminum and fluoride ions (Figure 3, FA). As can be inferred from the corresponding ^{27}Al NMR spectrum of this solution (see next section), only 7.6% of the added pseudoboehmite is detected. Also, from the ^{19}F NMR spectrum,

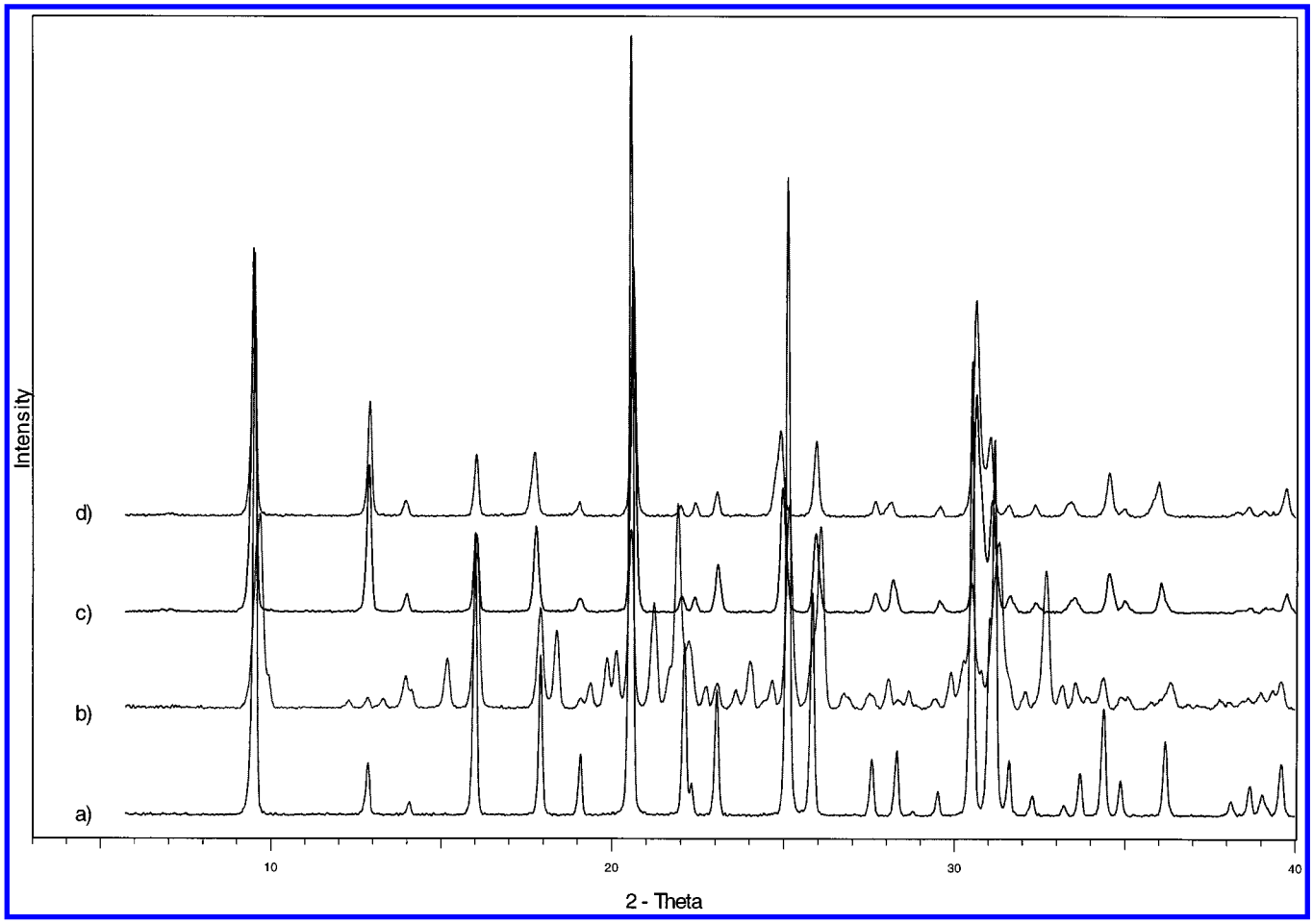

Figure 1. Typical X-ray patterns of the synthesized samples: (a) as-synthesized trigonal SAPO-34 prepared in the absence of HF; (b) as-synthesized trigonal and triclinic SAPO-34 prepared in the presence of HF; (c) calcination of (a) at 580 °C in air; (d) calcination of (b) at 580 °C in air.

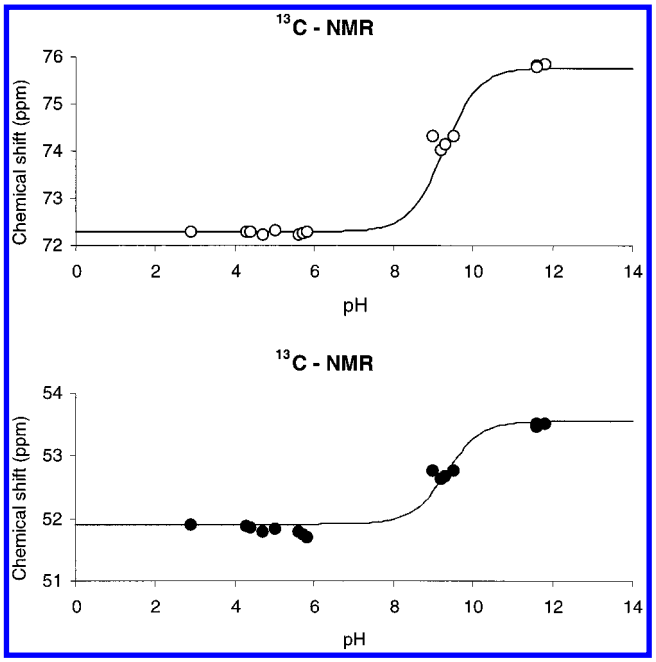

Figure 2. ^{13}C NMR chemical shift of the two different carbon groups in morpholine for all the morpholine-containing mixtures as a function of pH. The fitted line represents the model for pH dependence developed by Hansen et al.[38]

only 60% of the initial amount of added F is detected, suggesting that the residual 40% is precipitated out of the solution or made unobservable by exchange processes.

TABLE 3: Previous Published ^{19}F NMR Chemical Shifts[a] for Some Two-Component Fluoride-Containing Species

species	chemical shift (ppm)	ref
AlF^{2+}	−156.1	18
AlF_2^+	−155.6	18
AlF_3	−154.4	18
AlF_4^-	−153.3	18
AlF_5^{2-}	−153.1	18
AlF_6^{3-}	>−153.1[b]	18
$AlOHF_x$	−152.6	19
$AlOH_2F_x$	−152.3	19
HF	−158.6	39
HF_2^-	−148.5	39
F^-	−116.0	39
SiF_6^{2-}	−128.2	20
P−Al−F[c]	−140 to −150	23, 34

[a] Relative to $CFCl_3$. [b] Only observable at low temperature. [c] Unspecified aluminophosphate−fluoride complexes.

If it is assumed that the observed ^{27}Al and ^{19}F NMR signal intensities represent quantitatively the total amount of dissolved species in solution, the concentration of the individual species can be calculated as described in ref 38. This calculation ($[Al]_0 = 0.15$ M, $[F]_0 = 0.60$ M; pH = 4.2) gives $[AlF_3] = 0.03$ M, $[AlF_4^-] = 0.095$ M and $[AlF_5^{2-}] = 0.022$ M where [X] denotes the concentration of species X and $[X]_0$ represents the initial concentration. Increasing $[F]_0$ in the calculation from 0.6 to 1.0 M results in a significant amount of F^- (0.16 M), which should result in a sharp peak at $\delta = -116$ ppm. However, no such peak can be seen in the spectrum. Thus, the observed peaks are assigned to $AlF_{3(aq)}$ and AlF_4^-/AlF_5^{2-} complexes, respectively

TABLE 4: ^{19}F NMR Chemical Shifts[a] and Assignment of the Signals from This Work

		F^-		SiF_6^{2-}		$F^-/HF_2^-/HF$		P−Al−F		AlF_4^-/AlF_5^{2-}		AlF_3		HF				
	code	pH	δ_1	ΔV_{ppm}	δ_2	ΔV_{ppm}	δ_3	ΔV_{ppm}	δ_4	ΔV_{ppm}	δ_5	ΔV_{ppm}	δ_6	ΔV_{ppm}	δ_7	ΔV_{ppm}	$I_{observed}$	$I_{expected}$	% visible	species
1	F	1.7													−158.73	0.04	115	163	70.4	HF
2	FA	4.2									−152.78	0.62	−154.01	*b*			88	150	58.7	AlF_4^-/AlF_5^{2-}, AlF_3
3	FS	2.0			−127.29	0.89											106	133	79.6	SiF_6^{2-}
4	FP	1.6													−158.93	0.04	127	147	86.2	HF
5	FM	9.2	−115.93	0.04													141	141	100.0	F^-
6	FAS	3.9			−127.33	1.25					−125.95	0.74	−154.18	0.44			96	147	65.2	SiF_6^{2-}, AlF_4^-/AlF_5^{2-}, AlF_3
7	FAP	1.8							−151.21	2.58	−152.97	*b*	−153.88	*b*			95	134	70.7	P−Al−F, AlF_4^-/AlF_5^{2-}, AlF_3
8	FAM	9.5	−116.11	1.14					−149.12	3.19							113	130	86.9	F^-, AlF_5^{2-}/AlF_6^{3-}
9	FSP	1.5			−127.05	0.94											106	138	76.7	SiF_6^{2-}
10	FSM	9.3	−116.00	0.04													129	135	95.3	F^-
11	FPM	3.5					−142.71	0.05									119	128	93.3	F^-/HF_2^-/HF exchange
12	FASP	1.7			−127.21	1.51			−151.08	4.20	−152.93	*b*	−153.97	*b*			88	130	67.9	SiF_6^{2-}, P−Al−F, AlF_4^-/AlF_5^{2-}, AlF_3
13	FASM	9.3	−116.08	0.46													96	125	77.1	F^-
14	FAPM	4.8							−147.40	6.79							86	118	73.2	P−Al−F
15	FSPM	2.7			−127.35	0.06											120	123	97.5	SiF_6^{2-}
16	FASPM	5.6							−146.11	7.70							86	114	75.8	P−Al−F

[a] Relative to $CFCl_3$. [b] Narrow peaks, not possible to determine the width due to the overlap with other peaks/background.

(from Sur and Bryant,[18] $\delta = -154.4$, -153.3, and -153.1 ppm), where the two latter peaks overlap. Calculated concentrations of the different species as a function of pH (from tabulated equilibrium constants[34,40]) are given in Figure 4A (^{19}F NMR) and Figure 4B (^{27}Al NMR), respectively. The concentrations $[Al]_0$ and $[F]_0$ applied in these calculations represent average values of that present in the mixtures examined in this work. One question remains, what fluoride-containing species represent the 40% nonobservable ^{19}F NMR signal intensity? Most probably, it is due to precipitation ($Al(OH,F)_3$).

The combination of Ludox and HF gives, as expected,[20] a single resonance peak at $\delta = -127.3$ ppm and is assigned to SiF_6^{2-} (Figure 3, FS).

No interaction between phosphoric acid and HF (Figure 3, FP) is observed. Within the concentration range studied, this is in agreement with Ames et al.[21] The spectrum is therefore comparable to pure diluted HF (Figure 3, F).

The addition of HF to morpholine in surplus results in a single peak at $\delta = -115.9$ ppm (Figure 3, FM), and it is assigned to F^-. The concentrations of HF and HF_2^- at this pH (=9.2) are calculated to be less than 10^{-6} M and thus, have no effect on the chemical shift even under fast exchange conditions.

Mixtures 6−11 (Table 2) are all three-component systems (in addition to water). The peak assignments of these spectra can in most cases be made from the corresponding NMR spectra of the simpler two-component systems. In the FAS mixture, fluoride ions react both with silica and aluminum to form SiF_6^{2-}, AlF_3, and AlF_4^-/AlF_5^{2-} complexes (Figure 3, FAS). From intensity measurements it seems that the formation of SiF_6^{2-} is preferred over the formation of AlF_x^{+3-x} complexes. However, this will certainly be dependent on the solubility (and the particle sizes) of the respective reagents. Moreover, comparing this spectrum with that obtained from the FA mixture (Figure 3, FA), it is evident that the average number of fluoride ligands coordinated to aluminum is reduced. This is consistent with model calculations and is due to the reduced amount of available fluoride, caused by the competitive complexion of SiF_6^{2-}.

In addition to the signals originating from AlF_x^{+3-x} complexes, a broad signal outside the chemical shift region expected for AlF_x^{+3-x} complexes can be observed in the FAP mixture (Figure 3, FAP). This is rationalized by the formation of aluminophosphate−fluoride (P−Al−F) complexes, in which aluminum is coordinated to both fluoride and phosphate ligands. Such species have been reported in earlier NMR investigations but are not identified.[23,34] Intensity measurements indicate that ~95% of the observable fluoride is incorporated in the P−Al−F complexes.

When morpholine is added to the FA mixture, two signals appear (Figure 3, FAM). The first is uniquely assigned to F^- ($\delta = -116.1$ ppm). The weaker and much broader resonance band located at $\delta = -149.1$ ppm is tentatively assigned to AlF_x^{+3-x} species. Under slow exchange conditions, these AlF_x^{+3-x} complexes resonate at approximately $\delta = -153$ (1 ppm, but may shift toward a lower magnetic field if intermediate exchange rate processes take place. Due to the surplus of F^- in the solution, such exchange processes are likely. Setting [Al] = 0.0054 M, [F] = 0.60 M, and pH = 9.5 (from NMR intensity determination and pH measurements), the actual composition was determined by model calculations to be $[F^-] = 0.57$ M, $[AlF_5^{2-}] = 0.0019$ M, and $[AlF_6^{3-}] = 0.0033$ M. Thus, it is expect to observe F^-, AlF_5^{2-} and AlF_6^{3-} in the intensity ratio 60:1:2. If the smaller peak is assumed to originate from the

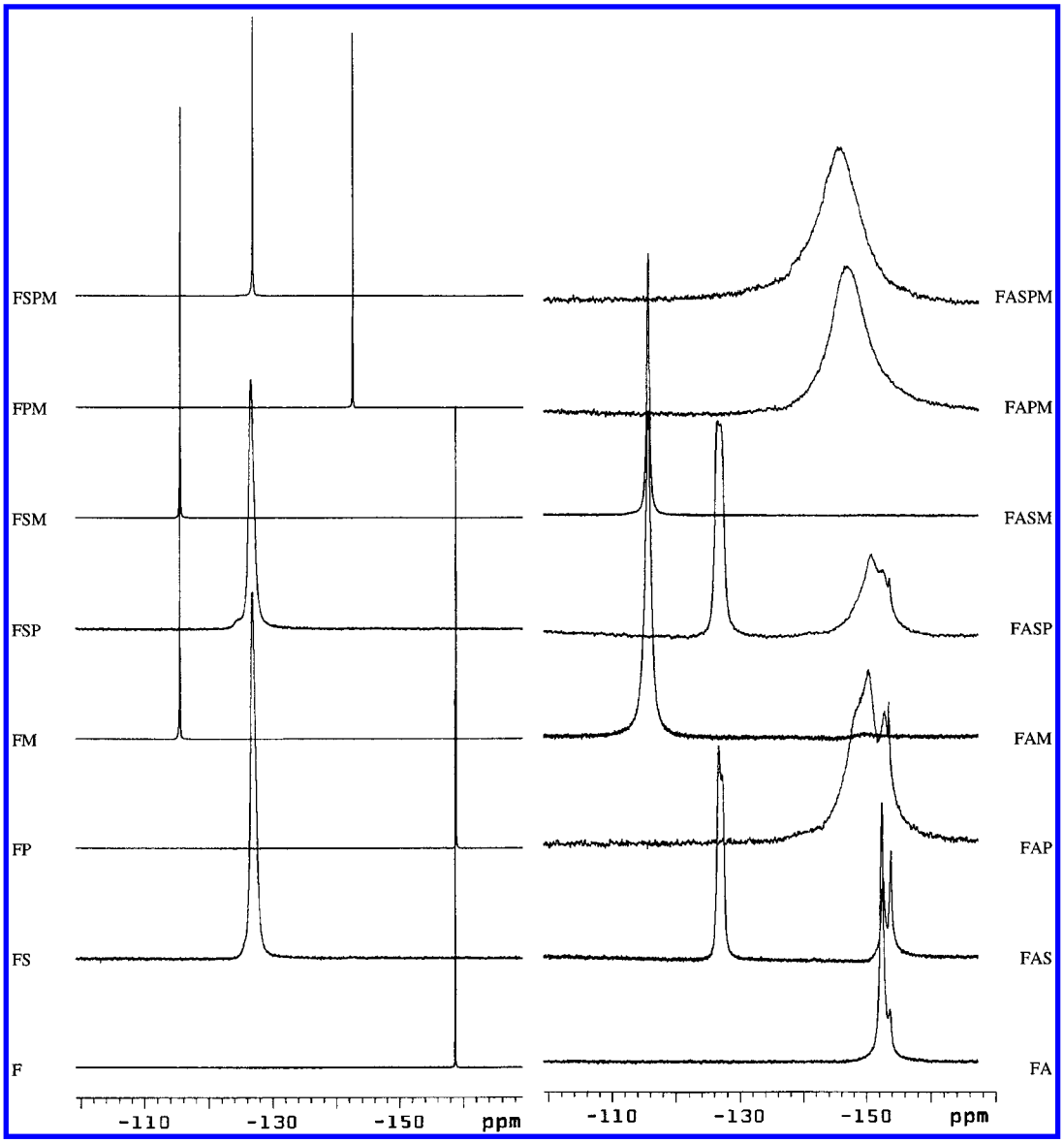

Figure 3. Obtained ^{19}F NMR spectra (for representative intensity measurements see Table 4).

overlap of the two latter species, this ratio is in excellent agreement with observation, 70:3. The broad peak is therefore assigned to the AlF_5^{2-}/AlF_6^{3-} complexes.

Adding phosphoric acid to the FS mixture does not reveal any significant change in the ^{19}F NMR chemical shift (Figure 3, FS and FSP), nor does addition of Ludox to the FM mixture (Figure 3, FM and FSM). The peaks observed in the FSP and FSM mixtures are therefore assigned to SiF_6^{2-} and F^-, respectively.

The FPM mixture gives a single resonance peak at $\delta = -142.7$ ppm (pH $= 3.25 \pm 0.25$, Figure 3, FPM). The model calculation results in the following concentrations: $[F^-] = 0.33$ M, $[HF_2^-] = 0.09$ M, and $[HF] = 0.18$ M. Assuming these species to be in fast exchange, a chemical shift of $\delta = -141 \pm 4$ ppm is predicted (within the specified pH range), which is in excellent agreement with the observed chemical shift ($\delta = -142.71$ ppm). The peak is therefore assigned to $F^-/HF_2^-/HF$ species in fast exchange.

Mixtures 12−15 (Table 2) are all four-component systems (in addition to water). In addition to SiF_6^{2-}, it is possible to observe one broad resolved resonance band in the FASP mixture (Figure 3, FASP). Except for the former peak, the spectrum resembles that observed for the FAP mixture (Figure 3, FAP). Curve-fitting analysis suggests that the major peaks originate from P−Al−F complexes. In addition, the two other smaller resonances can be identified as the complexes AlF_4^-/AlF_5^{2-} and AlF_3 ($\delta = -152.9$ and -154.0 ppm).

Excluding phosphoric acid from the final gel results in only one signal assigned to F^- ($\delta = -116.1$ ppm, Figure 3, FASM), which is rationalized according to the relatively low solubility of pseudoboehmite, besides the low formation of SiF_6^{2-} at this pH (=9.3). This is in agreement with investigations reported by Martinez et al.[19] and by Hansen et al.,[38] where only free fluoride was observed at pH > 7. However, this observation is in contrast to that obtained from the FAM mixture where some AlF_6^{3-}/AlF_5^{2-} was observed and according to the model calculations (Figure 4A). This is explained by a broadening of the resonance signal upon addition of Ludox, resulting in an increased viscosity.

Preparing the gel without Ludox gives a broad, symmetric resonance band at $\delta = -147.4$ ppm (Figure 3, FAPM). This is well outside the expected chemical shift range of AlF_x^{+3-x}, suggesting that this resonance band represents aluminophosphate−fluoride complexes. The broadening is most likely the result of overlap of several different resonance peaks.

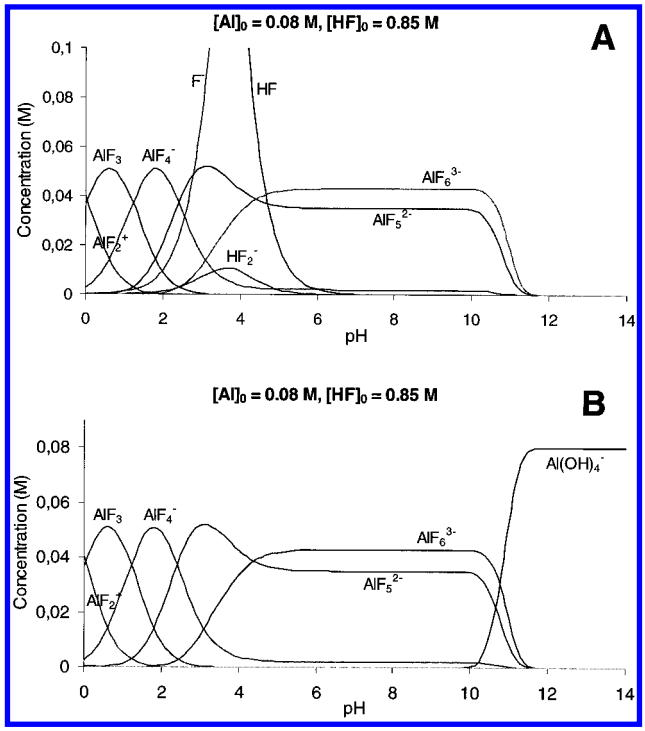

Figure 4. Calculated concentrations vs pH of the different species present at equilibrium in a mixture containing aluminum and fluoride ions at concentrations representative for the mixtures analyzed in this work. (A) represents the species to be observed with ^{19}F NMR and (B) with ^{27}Al NMR.

Excluding aluminum from the mixture gives a single resonance line (Figure 3, FSPM), which is assigned to SiF_6^{2-} (−127.4 ppm).

The FASPM mixture contains all species necessary to form SAPO-34. Only a single, broad (∼7.7 ppm) band at $\delta = -146.1$ ppm is observed (Figure 3, FASPM). This severe broadening is most likely the result of several overlapping peaks, but may also be related to the higher viscosity of the gel. The peak is nearly symmetric, revealing only a small low-field shoulder. From the relatively high pH (=5.6), no formation of SiF_6^{2-} is expected. On the other hand, previous results obtained in this work suggest formation of Al−F complexes, but such species cannot be uniquely identified (most probably due to broadening and overlap). The spectrum is therefore assigned according to the FAPM mixture.

A comparison of the observed total ^{19}F NMR signal intensity of the different mixtures in the presence and absence of pseudoboehmite shows an interesting trend (Figure 5). Addition of pseudoboehmite results in a general reduction in signal intensity and most probably originate from precipitation of some poorly soluble amorphous (from XRD) Al−F containg species.

Aluminum Interactions Observed by ^{27}Al NMR. The ^{27}Al NMR spectra contain in general little fine structure (Figure 6). For example, it has not been possible to separate peaks corresponding to the different AlF_x^{+3-x} complexes for $x > 2$. However, it is possible to provide some qualitative information about the distribution and composition of the various species present in the solutions. In addition, some quantitative information regarding the total Al content in the solution phase may be extracted. The possibility that other resonance peaks are broadened beyond detection cannot be ruled out.

Several explanations for the severe line broadening (∼6−18 ppm) observed when pseudoboehmite is used as an Al source, relative to the $Al(NO_3)_3$ reference (0.07 ppm), are feasible: (1) a decrease in the symmetry of the ligand field; (2) overlapping

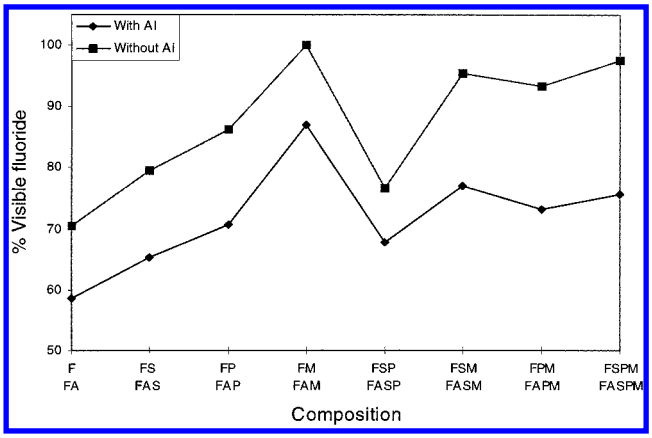

Figure 5. Correlation between visible fluorides for the mixtures, in the presence and absence of aluminum. The lower labels on the *x*-axis represent mixtures with pseudoboehmite, while the upper ones represent the same mixtures without pseudoboehmite. The FM mixture is used as reference for % visible fluoride because it gives the highest level of observable flour signal.

peaks; (3) increased viscosity and/or Al concentration;[26] (4) presence of a coexisting solid phase (nondissolved pseudoboehmite, precipitated $Al(OH,F)_3$, etc.). Narrower peaks may be obtained by centrifuging the mixtures prior to NMR sampling. However, since the main goal of this investigation is to establish an in situ procedure to enable the nucleation and crystallization to be monitored as a function of reaction time, centrifugation is not desirable.

As a result of the poor solubility of pseudoboehmite, only solutions containing either fluoride and/or phosphate species are discussed. In the one-, two-, or three-component mixtures only containing aluminum, morpholine, and/or Ludox (in addition to water), no interactions are detected and only octahedral Al about $\delta \approx 0$ ppm are observed. The majority of the ^{27}Al NMR resonance peaks from the less complex mixtures can be assigned from the literature (Table 5) and are summarized in Table 6. The spectra are shown in Figure 6.

The NMR spectrum of the FA mixture is shown in Figure 6, FA. The broad peak (10.9 ppm) is symmetric and centered at $\delta = -0.35$ ppm. It appears from the small signal intensity that the solubility of the Al-source is rather limited (7.6 mol %). It is not possible to confirm the existence of the three different AlF_x^{+3-x} complexes ($x = 3-5$) that were observed by ^{19}F NMR (Figure 3, FA). The peak position confirms octahedral Al coordination.

No interaction between Al and Si in the AS mixture can be revealed; moreover, no aluminum signal is observed at all. Adding HF to this mixture, the spectrum is rather similar to that obtained from the FA mixture, except for a reduction in observed signal intensity in the former mixture (Figure 6, FAS and FA). This is rationalized according to a competitive formation of SiF_6^{2-}, resulting in a reduced solubility of pseudoboehmite. Furthermore, the formation of $Al(OSi)_x$ species could be expected in both mixtures (giving resonance peaks in the chemical shift range $\delta = 58-72$ ppm[14,16]) but cannot be uniquely assigned.

The AP mixture shows a symmetric ^{27}Al NMR peak at $\delta = -8.26$ ppm (Figure 6, AP). The pH suggests that this is within the first buffer region of phosphoric acid ($pK_{a1} = 2.12$), consequently, the free phosphoric acid is mainly present as a mixture of H_3PO_4 and $H_2PO_4^-$. An upfield shift in the ^{27}Al NMR resonance is thus expected since P-containing ligands are more electronegative than H_2O. On the basis of literature data[25,26] and ^{31}P NMR (discussed below), this resonance band is assigned

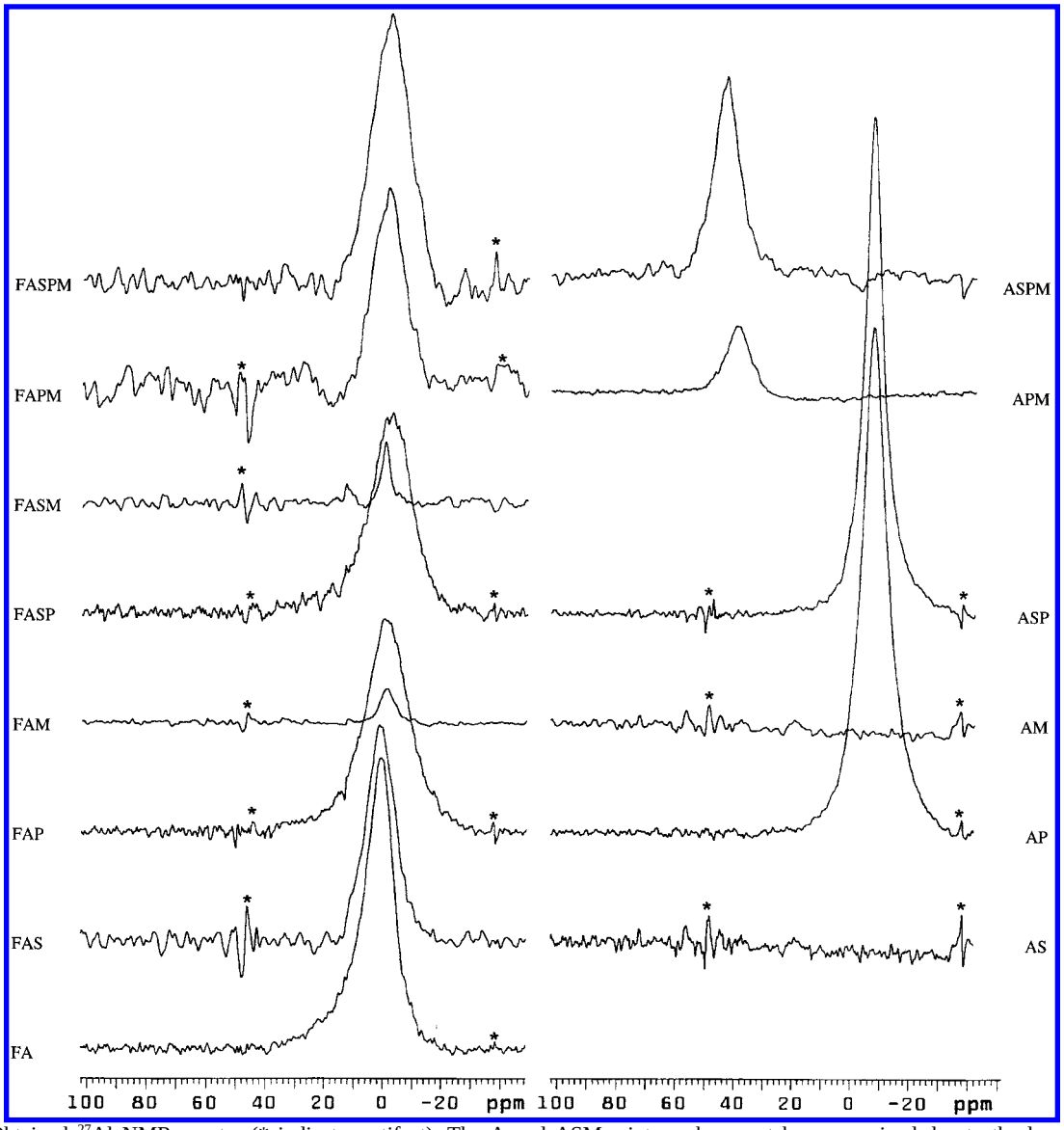

Figure 6. Obtained ^{27}Al NMR spectra (* indicates artifact). The A and ASM mixtures have not been examined due to the low solubility of pseudoboehmite; see Table 6 for representative intensity measurements.

to $[Al(H_2O)_4(H_3PO_4)_2]^{3+}$, $[Al(H_2O)_4(H_2PO_4)(H_3PO_4)]^{2+}$, and $[Al(H_2O)_4(H_2PO_4)_2]^{+}$ species, which all have chemical shifts between $\delta = -7.5$ and -9.0 ppm. Moreover, it is possible that more that two PO_4 tetrahedra are complexed to Al.

When adding hydrofluoric acid to this mixture, the resonance band is broadened and shifted downfield ($\delta = -3.9$ ppm; Figure 6, FAP). Except for changes in the chemical shift, the spectrum resembles those observed from the FA and FAS mixtures. ^{19}F NMR (Figure 3, FAP) suggests that the resonance band in the ^{27}Al NMR spectrum is composed of at least four different species: AlF_3, AlF_4^-/AlF_5^{2-}, and, most probably, at least one P−Al−F complex. From the ^{19}F NMR spectrum, it is assumed that the last species is the main Al-containing component in the solution phase (∼95%). Keeping in mind that neither the number of fluoride nor hydroxyl ligands coordinated to aluminum introduce any significant changes in the ^{27}Al NMR chemical shift,[38] suggests that the upfield shift in the ^{27}Al NMR spectrum (relative to the reference) is due to this phosphate ligand. In an earlier investigation, Wilson et al.[25] proposed that a species with an Al/P ratio = 1 is responsible for a peak located at $\delta \cong -3.6$ ppm. In addition, Miyajima et al.[28,29] have assigned one peak in this chemical shift region to Al complexed to polyphosphates, with only one phosphate-containing ligand coordinated to Al. Therefore, it is reasonable to suggest that only one phosphate-species is coordinated to Al. The exact composition of the complex is not known. However, combining all this information with that derived from ^{31}P NMR (discussed below) and the pH (=1.8), it is proposed that the complex is of the form $[Al(H_2O)_{5-x}(H_2PO_4)(F,OH)_x]^{+2-x}$.

Figure 6, ASP and FASP, shows the ^{27}Al NMR spectra of the final gels apart the structure-directing agent, in the absence and presence of HF. No differences are noticed from the Ludox free counterparts, indicating the absence of $Al(OSi)_x$ species. The ASP and FASP mixtures are therefore assigned according to the AP and FAP mixtures.

The AM and FAM mixtures are of particular interest because they may reveal some interaction between the structure-directing agent and the aluminum. In the former mixture, no signal was detected (Figure 6, AM). On the other hand, in the latter mixture, approximately 1 mol % of the Al was detected ($\delta \cong -1.8$ ppm), resulting in a rather poor signal-to-noise ratio (Figure 6, FAM). Most of the fluoride exists as F^-, although the ^{19}F NMR spectrum (Figure 3, FAM) and model calculation suggest that some AlF_5^{2-} and AlF_6^{3-} are also present in the mixture under these conditions (pH = 9.5). The peak is therefore assigned to

TABLE 5: Previous Published ^{27}Al NMR Chemical Shift Ranges[a] for Some Typical Aluminum Species

species	chemical shift range (ppm)	ref
$Al(OH)_4^-$ (i.e. Al(OSi))[b]	80−79.5	41, 42
$Al(OH)_3$	9.3	30
Al(1Si)[b]	70−72	14, 16
Al(2Si)[b]	66	14, 16
Al(3Si)[b]	61	14
Al(4Si)[b]	58	14
$Al(OH)_4^-$ bonded to HPO_4^{2-} ions	60−67	27
pentacoordinated Al bonded to HPO_4^{2-} ions	43−52	27
octahedral Al species bonded to HPO_4^{2-} ions	−20−30	27
$Al(H_2O)_6^{3+}$	0.0 to −1.0	23
Al_2P, where P most probably represents HPO_4^{2-}	−1.4	25
AlP, P most probably is $H_2PO_4^-$ and the Al/P ratio = 1	−3.2	25
$[Al(H_2O)_5(PO^-)]^{2+}$, where PO^- is polyphosphate	−3.2	28, 29
$[Al(H_2O)_5(H_3PO_4)_n]^{m+}$ ($n \geq 2$, m is undetermined)	−3 to −5	27
AlP_x, where P most probably is H_3PO_4	−6.2	25
$[Al(H_2O)_4(PO^-)_2]^+$, where PO^- is polyphosphate	−6.4	28, 29
$[Al(H_2O)_5(H_3PO_4)]^{3+}$	−6 to −7.5	27
AlP_x, where P most probably is $H_2PO_4^-$	−7.6	25
$[Al(H_2O)_5(H_2PO_4)]^{2+}$ and *trans*-$[Al(H_2O)_4(H_2PO_4)_2]^+$	−7.5 to −9	27
Al dimers bonded to phosphate ligands	−1 to −2	27
$[Al(H_2O)_3(PO^-)_3]^0$, where PO^- is polyphosphate	−9.6	28, 29

[a] Relative to 1.0 M $Al(H_2O)_6^{3+}$. [b] Highly alkaline solutions (pH ≥ 13).

these two latter species. Adding Ludox (Figure 6, FASM) does not alter the spectrum.

It appears from the titration curve of phosphoric acid (not shown here) that a significant amount of HPO_4^{2-} is formed when pH > 4.7. This must be taken into account when discussing the APM and FAPM mixtures (pH = 5.7 and 4.8, respectively). According to the investigation performed by Wilson et al.,[25] a resonance peak at $\delta \cong -1.4$ ppm, caused by octahedral Al coordinated to HPO_4^{2-}, is expected in this pH region. As can be inferred from the latter F-containing mixture, this is in good agreement with the obtained spectrum ($\delta = -1.73$ ppm; Figure 6, FAPM). Although the line width is narrower than that observed for the FAP and FASP mixtures, the peak is assigned to P−Al−F complexes, where the nature of the PO_4 ligands are assumed to be HPO_4^{2-}. Lack of any resonance peak about $\delta = 0$ ppm suggests that AlF_x^{+3-x} complexes are not present and is in agreement with ^{19}F NMR (Figure 3, FAPM).

For the former fluoride-free mixture (APM), this is not consistent with the obtained spectrum, where no distinct signal from octahedral Al can be observed (Figure 6, APM). Various reasons for this downfield shift may arise. First, it could be caused by the increase in pH from 2.2 to 5.7 upon addition of morpholine, thereby altering the coordination number. This has been suggested by Mortlock et al.,[27] who reported a peak within the range 43−52 ppm ($AlPO_4$ solution containing TMSOH), which they assigned to pentacoordinated Al bonded to HPO_4^{2-}. However, no such peak was detected in the work reported by Hansen et al.,[38] when systematically increasing the pH in a mixture of $Al(NO_3)_3$ and H_3PO_4 by adding NaOH. This rules out the possibility that the downfield shift is due to a pH effect alone.

For instance, Prasad et al.[30,31] have claimed that tetrahedral Al only appears in the gel after addition of the structure-directing agent. However, in the absence of phosphate species, Hansen et al. [30] have proposed that morpholine, as a structure-directing agent, is inactive at room temperature.

Another interpretation can be made from comparison of the ^{27}Al MAS NMR spectra of as-synthesized SAPO-34. Here, the framework AlO_4 tetrahedra gives a resonance peak at $\delta = 39$ ppm.[11,43] Therefore, regarding the intermediate pH (=5.7) in the APM mixture and the excellent agreement between the ^{27}Al NMR spectra of this mixture and the ^{27}Al MAS NMR of as-synthesized SAPO-34, it is appropriate to assign the peak to "tetrahedral Al". Moreover, the AlO_4 tetrahedra are coordinated to phosphate tetrahedra and morpholine is acting as a "coordination"-directing species.

One question remains to be answered; why is generation of tetrahedral Al not observed in the mixture containing hydrofluoric acid? This might be rationalized by the strong complexing character of the fluoride ions, resulting in octahedral Al coordination. ^{27}Al MAS NMR and structure analysis of as-synthesized SAPO-34 has shown that the structure contains such species.[43]

The ^{27}Al NMR spectra of the final gels are given in Figure 6, ASPM and FASPM. Except for an additional small downfield chemical shift ($\delta = 42.1$ ppm), no significant difference is observed when Ludox is added to the APM mixture. The final gel, in the absence of HF, is therefore assigned accordingly to the APM mixture.

The fluoride-containing final gel results in a rather broad peak (15.7 ppm) with an average chemical shift of approximately $\delta = -2.63$ ppm (Figure 6, FASPM). The peak is tentatively assigned to Al−F−P complexes. The increased gel viscosity may explain the broadening. It is assumed that AlF_x^{+3-x} complexes are not present (from ^{19}F NMR, Figure 3, FASPM).

Phosphate Interactions Observed by ^{31}P NMR. The proteolysis of an acid solution increases with dilution and is confirmed by ^{31}P NMR. The spectrum of an 85% H_3PO_4 solution gives rise to a single resonance peak at $\delta = 0.00$ ppm. Upon dilution with water, the signal shifts toward $\delta = 0.56$ ppm (the P mixture; Figure 7, P). When varying the pH in the range from 1 to 3.5, the concentration of H_3PO_4 and $H_2PO_4^-$ will change accordingly. Likewise, under fast exchange conditions, the ^{31}P chemical shift of the single resonance peak will be determined by the weighted average of the chemical shift of the two species, H_3PO_4 ($\delta = 0$ ppm[26]) and $H_2PO_4^-$. The chemical shift of the latter species is strongly dependent on the concentration; $\delta = 3.75$ and 0.25 ppm in 1.0 M H_2PO_4[26] and saturated NaH_2PO_4 solution,[44] respectively. The observed chemical shift when adding $AlCl_3$ to a saturated $H_2PO_4^-$ mixture is reported to be within the range 0.2 to −0.1 ppm.[25]

The ^{31}P NMR resonance peaks from the less complex mixtures are assigned from the literature (Table 7) and are summarized in Table 8. Within the examined concentration range, no interaction between phosphates and fluorides, silicates, and/or morpholine can be observed in any of the mixtures. The only ^{31}P NMR resonance peak detected in these mixtures is assigned to $H_3PO_4/H_2PO_4^-$. Some minor shift in the peak position may occur due to pH effects upon addition of HF or morpholine (Figure 7).

It has previously been noted that the solubility of the Al source is strongly dependent on the presence of H_3PO_4. Complex formation between Al and PO_4 species is therefore expected. Also, some octahedral P−Al−F complexes have been assigned from the ^{19}F and ^{27}Al NMR.

The ^{31}P NMR spectrum of the AP mixture reveals three distinct signals (Figure 7, AP). The low signal intensity could be due to precipitation; nevertheless, broadening beyond detection cannot be eliminated. The main peak ($\delta = -0.25$ ppm) is assigned to free $H_3PO_4/H_2PO_4^-$, while the two residual peaks

TABLE 6: ^{27}Al NMR Chemical Shift[a] and Assignment of the Signals from This Work

			tetrahedral Al		AlF_x^{+3-x}		P−Al−F		$[Al(H_2O)_{6-n}(H_{3-x}PO_4)_n]^{+3-xn}$					
	code	pH	δ_1	ΔV_{ppm}	δ_2	ΔV_{ppm}	δ_3	ΔV_{ppm}	δ_4	ΔV_{ppm}	$I_{observed}$	$I_{expected}$	% visible	species[b]
2	FA	4.2			−0.35	10.9					351	2246	7.6	AlF_3, AlF_4^-/AlF_5^{2-}
6	FAS	3.9			1.12	11.5					256	2136	5.8	AlF_3, AlF_4^-/AlF_5^{2-}
7	FAP	1.8					−3.87	22.7			287	2013	6.9	P−Al−F, AlF_3, AlF_4^-/AlF_5^{2-}
8	FAM	9.5			−1.83	5.9					15	1959	0.37	AlF_5^{2-}/AlF_6^{3-}
12	FASP	1.7					−3.69	18.0			267	2017	7.2	P−Al−F, AlF_3, AlF_4^-/AlF_5^{2-}
13	FASM	9.3			−0.75	3.2					10	1875	0.26	AlF_5^{2-}/AlF_6^{3-}
14	FAPM	4.8					−1.73	11.8			216	1791	5.9	P−Al−F
16	FASPM	5.6					−2.63	15.7			352	1713	10.0	P−Al−F
18	A													not examined
22	AS	7.0												no observations
23	AP	2.4							−8.26	9.9	767	2269	16.4	$[Al(H_2O)_4(H_3PO_4)_2]^{3+}$, $[Al(H_2O)_4(H_2PO_4)_2]^+$, and/or $[Al(H_2O)_4(H_2PO_4)(H_3PO_4)]^{2+}$
24	AM	11.6												no observations
28	ASP	2.1							−8.36	7.1	623	2002	15.1	$[Al(H_2O)_4(H_3PO_4)_2]^{3+}$, $[Al(H_2O)_4(H_2PO_4)_2]^+$, and/or $[Al(H_2O)_4(H_2PO_4)(H_3PO_4)]^{2+}$
29	ASM													not examined
30	APM	5.7	38 ± 2	10.4							86	1841	2.3	tetrahedral Al
32	ASPM	5.8	42.1	9.9							186	1774	5.1	tetrahedral Al

[a] Relative to 1.0 M $Al(NO_3)_{3\,(aq)}$. [b] $[Al(H_2O)_6]^{3+}$ is omitted from the table, but does probably exist in small quantities in all the mixtures where a resonance peak is observed around 0 ppm.

are assigned to $[Al(H_2O)_{6-n}(H_2PO_4)_n]^{+3-n}$ ($\delta = -7.83$ ppm), $[Al(H_2O)_{6-n}(H_3PO_4)_n]^{3+}$ ($\delta = -12.29$ ppm), and/or $(Al(H_2O)_{6-n-m}(H_2PO_4)_n(H_3PO_4)_m]^{+3-n}$ ($\delta = -7.83$ and -12.29 ppm).[26] The number of PO_4 ligands, *n*, is determined to be at least 2 from ^{27}Al NMR (Figure 6, AP). It may also be possible that the latter two peaks originate from dimeric aluminum, bonded to $H_2PO_4^-$ and H_3PO_4, respectively. However, this is ruled out from the ^{27}Al NMR results and the Löwensteins rule,[45] in which an Al−O−Al bond is energetically unfavorable in the final solid product.

Addition of HF results in the disappearance of the two latter peaks. The main peak ($\delta = 0.09$ ppm, Figure 7, FAP) is still assigned to the $H_2PO_4^-/H_3PO_4$ species. In addition, one smaller and broader peak is observed at $\delta = -6.5$ ppm. ^{31}P NMR gives information about the nature of the ligands but tells nothing about the coordination number. The latter peak may therefore be expected to originate from $H_2PO_4^-$ coordinated to Al.[27] Taking into account the ^{19}F and ^{27}Al NMR results mentioned above, the composition is anticipated to be of the form $[Al(H_2O)_{5-x}(H_2PO_4)(F,OH)_x]^{+2-x}$.

The changes in chemical shift of the two peaks from the FAP mixture have been recorded as function of time. The result is summarized in Figure 8. The intensity of the smaller peak increases with time at the expense of the main peak and converges toward 25% of the total signal intensity approximately after 4 h. This indicates that more of the Al is present in the solution phase, complexed with PO_4 species, with increasing time of aging. Line broadening is observed for both peaks, which is consistent with an increasing viscosity and Al concentration.[26] The average chemical shifts of the two peaks are $\delta = 0.10 \pm 0.13$ and $\delta = -6.52 \pm 0.65$ ppm. Since no systematic variation in δ vs time was observed, the standard deviations were estimated from simple statistical evaluation of the time-resolved spectra.

No difference in the ^{31}P NMR spectrum is expected when adding Ludox to the AP and FAP mixture, which is in agreement with the observation (Figure 7, ASP and FASP). These mixtures are therefore assigned according to the AP and FAP mixture.

The shapes of the ^{31}P NMR spectra of the APM and FAPM mixtures are identical (Figure 7, APM and FAPM). Only one narrow peak assigned to $H_3PO_4/H_2PO_4^-$ is observed. The shift toward lower field compared to the FAP and FASP mixtures is related to the increase in pH from about 2 to 5 upon addition of morpholine. The absence of the two peaks located at $\delta = -7.7$ and $\delta = -12.3$ ppm (AP and ASP mixtures) can be explained in (at least) two ways. First, comparing the pH of these two latter mixtures (2.4 and 2.1, respectively) with that obtained for the APM mixture (5.7) suggests changes in the nature of the PO_4 ligands. Moreover, the small amount of observable Al might indicate that these latter peaks are absent due to precipitation. Second, it has been concluded that morpholine behaves as a "coordination" directing species in the APM and ASPM mixtures, prohibiting formation of $[Al(H_2O)_{6-x}(H_2PO_4)_x]^{+3-x}$ and $[Al(H_2O)_{6-x}(H_3PO_4)_x]^{3+}$. The latter two peaks may therefore be absent due to broadening of the signal, which is caused by reduced symmetry around the Al tetrahedra (i.e. comparable with the 12 unobservable (by NMR) octahedral Al coordinated around the observable central tetrahedral Al in the "keggin" structure[46]). A similar observation has been reported by Marcuccilli-Hoffner in the preparation of $AlPO_4$-11.[34]

In the corresponding HF-containing mixtures, no sign of tetrahedral Al was detected (^{27}Al NMR), which was assumed to be due to the complexing character of the fluoride ions. However, the ^{31}P NMR spectra are identical (in the presence and absence of HF), suggesting identical phosphate environments.

The ^{31}P NMR spectrum of the final gel, in the absence of HF, is displayed in Figure 7, ASPM. Only one peak at $\delta = -0.29$ ppm is observed. This spectrum resembles that observed for the APM mixture, which is not surprising since their pHs are almost equal (5.7 and 5.8). In addition, there is no evidence for any interaction between Ludox and PO_4 species.

Figure 7, FASPM, shows the ^{31}P NMR spectrum of the final gel in the presence of HF. Upon comparison with the corresponding Ludox free mixture (FAPM), one main distinction can be made. Two peaks are detected, a main peak assigned to the $H_3PO_4/H_2PO_4^-$ ($\delta = 0.35$ ppm) and a smaller peak most probably related to the interaction between PO_4 species and Al ($\delta = -3.65$ ppm). The ^{19}F NMR spectrum suggests the presence of P−Al−F complexes. A corresponding peak was reported by Marcuccilli-Hoffner,[34] although the composition of the complex was not determined.

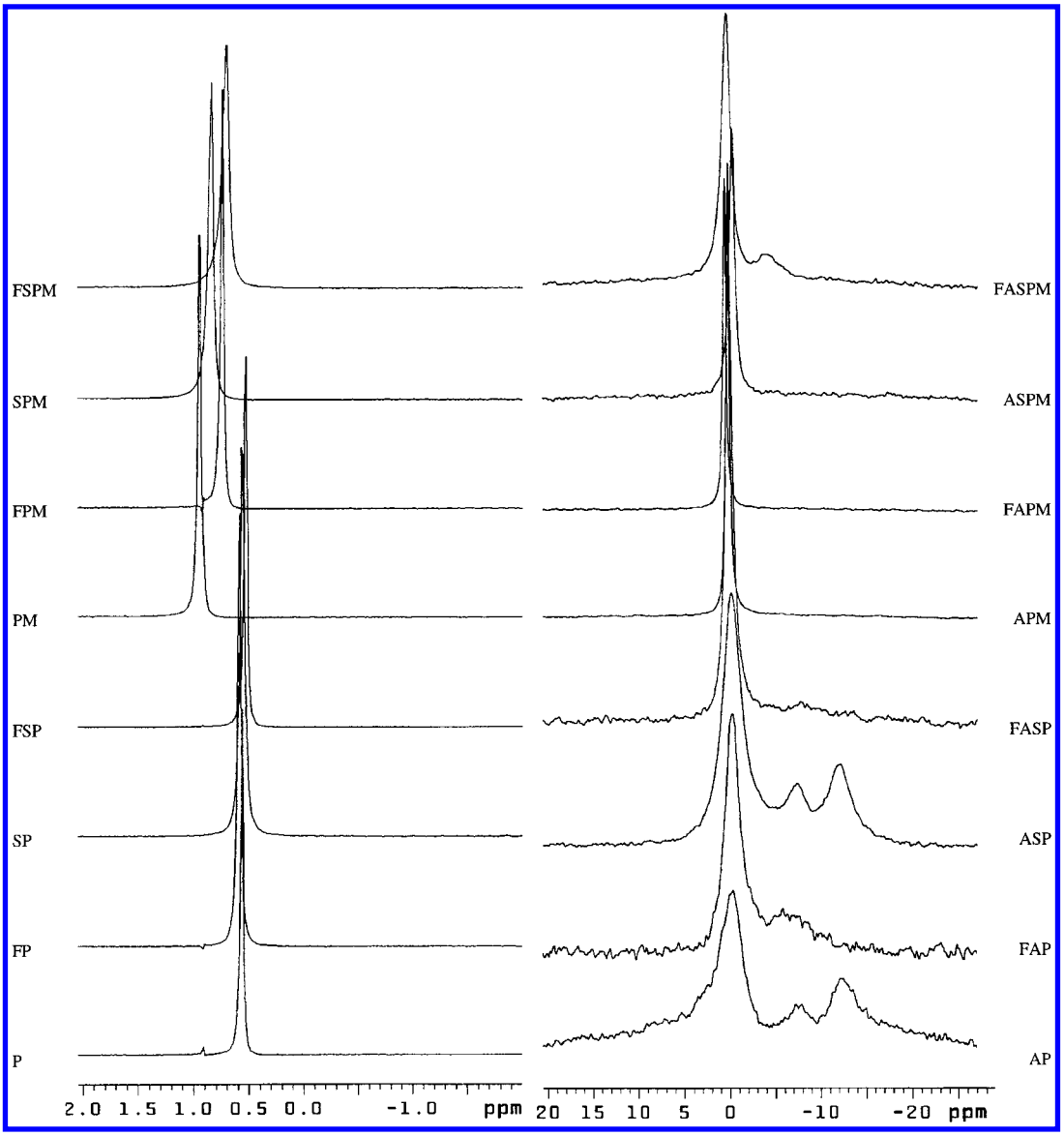

Figure 7. Obtained ^{31}P NMR spectra (for representative intensity measurements see Table 8).

It has previously been reported that the pH may change by 3−4 units during the early stage of the synthesis reaction.[7,47] As shown in this work, this significantly affects the type and concentration of species formed. This will be the subject for future studies, in which the formation of complexes will be monitored as a function of reaction time under synthesis conditions, the pH of the crystallizing gel being monitored using morpholine. The kinetic parameters obtained from NMR experiments will then be related to the kinetic information collected from ex situ studies of syntheses performed in a 1 L autoclave equipped with an in situ sampler**.**

Conclusion

Multinuclear, high-resolution NMR spectroscopy has been applied to identify the large number of complexes present in mixtures prepared from all possible combinations of hydrofluoric acid, Ludox, pseudoboehmite, phosphoric acid and morpholine. The nature and numbers of complexes present are shown to be dependent on the pH and concentration.

The ^{13}C and ^{1}H NMR chemical shift model developed by Hansen et al.[38] for monitoring the pH in situ has been shown to be reliable. Since the pH in typical $AlPO_4$ and SAPO syntheses increases from approximately 6 to about 10 under an ordinary

TABLE 7: Previous Published ^{31}P NMR Chemical Shift Ranges[a] for Some Typical Phosphate-Containing Species

species	chemical shift range (ppm)	ref
PO_4^{3-}	8.70[b]	26
HPO_4^{2-}	6.25[b]	26
$H_2PO_4^-$	3.75[b]	26
H_3PO_4	0.000[c]	26
HPO_4^{2-} ions bonded to Al species	1−6	27
free PO_4^{3-}, HPO_4^{2-}, or $H_2PO_4^-$ ions bonded to Al species	3−8	27
$H_2PO_4^-$ ions bonded to Al dimers	−6 to −8	27
$[Al(H_2O)_5(H_2PO_4)]^{2+}$	−7 to −10	27
trans-$[Al(H_2O)_4(H_2PO_4)_2]^+$	−7 to −10	27
$[Al(H_2O)_5(H_3PO_4)]^{3+}$	−11.5 to −14	27
trans-$[Al(H_2O)_4(H_3PO_4)_2]^{3+}$	−12.60[b]	26
trans-$[Al(H_2O)_4(H_2PO_4)(H_3PO_4)]^{2+}$ [d]	−9.47 and −12.60[b]	26
H_3PO_4 molecules bonded to Al dimers	−12 to −15	27
P nuclei bridging Al dimers	−14 to −15	27
P nuclei bridging Al monomers	−15 to −22	27

[a] Relative to 85% H_3PO_4. [b] Calculated using the MNDO (modified neglect of differential overlap) Hamiltonian (1 M solution).[26] [c] A downfield shift appears when concentration is reduced below 85%. [d] Each phosphate group originates in a ^{31}P NMR resonance.

TABLE 8: ^{31}P NMR Chemical Shifts[a] and Assignment of the Signals from This Work

	code	pH	$H_3PO_4/H_2PO_4^-$		P−Al−F		$[Al(H_2O)_{6-x}(H_2PO_4)_x]^{+3-x}$		$[Al(H_2O)_{6-x}(H_3PO_4)_x]^{+3}$		$I_{observed}$	$I_{expected}$	% visible	species[b]
			δ_1	ΔV_{ppm}	δ_2	ΔV_{ppm}	δ_3	ΔV_{ppm}	δ_4	ΔV_{ppm}				
4	FP	1.6	0.59	0.04							72	129	55.8	$H_3PO_4/H_2PO_4^-$
7	FAP	1.8	0.09	1.94	−6.46	4.13					17	120	14.4	$H_3PO_4/H_2PO_4^-$, $[Al(H_2O)_{5-x}(H_2PO_4)(F,OH)_x]^{+2-x}$
9	FSP	1.5	0.51	0.22							136	123	110.5	$H_3PO_4/H_2PO_4^-$
11	FPM	3.5	0.73	0.22							70	113	61.6	$H_3PO_4/H_2PO_4^-$
12	FASP	1.7	−0.12	0.93	−7.73	1.98					25	115	21.8	$H_3PO_4/H_2PO_4^-$, $[Al(H_2O)_{5-x}(H_2PO_4)(F,OH)_x]^{+2-x}$
14	FAPM	4.8	0.30	1.09	*b*						41	105	39.0	$H_3PO_4/H_2PO_4^-$
15	FSPM	2.9	0.70	0.27							63	109	58.0	$H_3PO_4/H_2PO_4^-$
16	FASPM	5.6	0.35	1.16	−3.79	2.47					39	102	36.6	$H_3PO_4/H_2PO_4^-$, $[Al(H_2O)_{5-x}(H_2PO_4)(F,OH)_x]^{+2-x}$
20	P	1.6	0.560	0.06							134	134	100.0	$H_3PO_4/H_2PO_4^-$
23	AP	2.4	−0.25	3.62			−7.83	2.89	−12.93	5.40	46	133	34.5	$H_3PO_4/H_2PO_4^-$, $[Al(H_2O)_4(H_3PO_4)_2]^{3+}$, $[Al(H_2O)_4(H_2PO_4)_2]^+$, and/or $[Al(H_2O)_4(H_2PO_4)(H_2PO_4)]^{2+}$
25	SP	1.8	0.56	0.05							71	127	56.0	$H_3PO_4/H_2PO_4^-$
27	PM	5.0	0.94	0.23							94	117	80.4	$H_3PO_4/H_2PO_4^-$
28	ASP	2.1	−0.04	2.57			−7.37	2.48	−12.29	3.88	106	118	89.9	$H_3PO_4/H_2PO_4^-$, $[Al(H_2O)_4(H_3PO_4)_2]^{3+}$, $[Al(H_2O)_4(H_2PO_4)_2]^+$, and/or $[Al(H_2O)_4(H_2PO_4)]^{2+}$
30	APM	5.7	0.19	0.43							77	109	70.6	$H_3PO_4/H_2PO_4^-$, PO_4 tetrahedra coordinated to tetrahedral Al
31	SPM	4.4	0.84	0.25							106	112	95.0	$H_3PO_4/H_2PO_4^-$
32	ASPM	5.8	−0.29	0.73							21	105	19.7	$H_3PO_4/H_2PO_4^-$, PO_4 tetrahedral coordinated to tetrahedral Al

[a] Relative to 85% H_3PO_4. [b] Peak expected to be observed after aging.

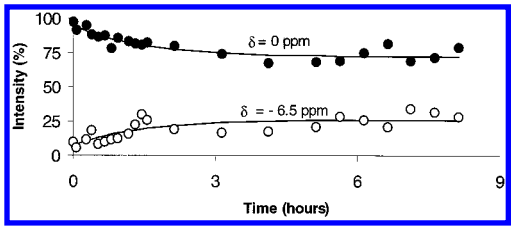

Figure 8. Changes in the total intensity of the two major ^{31}P NMR peaks observed in the FAP mixture as a function of time.

synthesis, this is an interesting aspect that can be utilized in further high-temperature studies.

Some interesting trends when adding the different ingredients to the simpler mixtures have been observed. Especially the addition of H_3PO_4, HF, or both reagents to the Al source gave some interesting results. Within the concentration range investigated, no direct interaction between fluoride and phosphate was detected, but both species have been shown to complex with octahedral Al in acidic environments. Only octahedral Al was detected in the presence of fluoride ions. The number of F ligands has been shown to be dependent on the fluoride and aluminum concentration. Addition of Ludox gave rise to competitive complexion of SiF_6^{2-} (from ^{19}F NMR, in the pH range 1.5−5.5).

The main ^{31}P NMR peak observed in all the phosphate-containing mixtures has been assigned to the rapid exchange between H_3PO_4 and $H_2PO_4^-$ ($\delta = 0.9$ to -0.3 ppm), where the chemical shift was dependent on both the PO_4 concentration and the pH. Two additional PO_4 species are observed when pseudoboehmite is present (in the absence of HF and morpholine): $[Al(H_2O)_{6-n}(H_2PO_4)_n]^{+3-n}$ ($\delta = -7.8$ ppm) and $[Al(H_2O)_{6-n}(H_3PO_4)_n]^{3+}$ ($\delta = -12.3$ ppm), where $n \geq 2$ (from ^{27}Al NMR). These species were eliminated after adding either HF or morpholine. The former case gave rise to P−Al−F complexes, the composition of which was suggested to be of the form $[Al(H_2O)_{5-x}(H_2PO_4)(F,OH)_x]^{+2-x}$. In addition, AlF_x^{+3-x} complexes ($3 \leq x \leq 6$) forms in the more acidic mixtures. In the latter case (adding morpholine), formation of tetrahedral Al was observed. Morpholine is therefore ascribed as an active "coordination"-directing species even at room temperature. Addition of HF to the APM mixture inhibited the formation of tetrahedral Al.

The time-resolved ^{31}P NMR spectra of the FAP mixture shows that kinetic information may be extracted by NMR during the time of aging.

The presence of fluoride results in an increasing pseudoboehmite solubility and reduced nucleation/crystallization time. The reduction in synthesis time may originate from the increased solubility of the aluminum source. Furthermore, addition of pseudoboehmite to fluoride-containing mixtures reduces the amount of visible fluoride, ascribed to precipitation or formation of low-symmetry complexes that are invisible to NMR. It should also be pointed out that free fluoride was totally absent due to complex formation in mixtures containing pseudoboehmite and/or Ludox. This reduces the hazard when handling these mixtures.

Acknowledgements. The authors would like to acknowledge the financial assistance from the Research Council of Norway and Norsk Hydro.

Note Added in Proof. Recently, new interesting and important results regarding the ^{31}P NMR assignments of aluminophosphate solutions have been obtained (Haouas, M. Etude RMN de la synthèse hydrothermale des aluminophosphates microporeux oxyfluorés: AlPO4, CJ2, ULM-3 et ULM-4.

Thèse, Université Louis Pasteur, Strasbourg, France, January, 1999). These ideas will be examined in a future NMR study of the SAPO-34 gels under hydrothermal conditions.

References and Notes

(1) Wilson, S. T.; Lok, M. B.; Messina, C. A.; Cannan, T. R.; Flanigen, E. M. *J. Am. Chem. Soc.* **1982**, *104*, 1146.

(2) Lok, M. B.; Messina, C. A.; Patton, R. L.; Gajek, R. T.; Cannan, T. R.; Flanigen, E. M. (a) U.S. Patent 4,440,871, April 3, 1984; (b) *J. Am. Chem. Soc.* **1984**, *106*, 6092.

(3) Haouas, M.; Gérardin, C.; Taulelle, F.; Estournes, C.; Loiseau, T.; Ferey, G. *J. Chim. Phys.* **1995**, *95*, 302.

(4) Norby, P. *Mater. Sci. Forum* **1996**, *228*, 147.

(5) Praksch, A. M.; Unnikrishnam, S. *Chem. Soc. Faraday* **1994**, *90*, 2291.

(6) Grinus, I.; Löffler, E.; Lohse, U.; Neissendorfer, F. *Collect. Czech.* **1992**, *57*, 946.

(7) Dumitriu, E.; Azzouz, A.; Hulea, V.; Lutic, D.; Kessler, H. *Microporous. Mater.* **1997**, *10*, 1.

(8) Chen, J. S.; Thomas, J. M. *Catal. Lett.* **1991**, *11*, 199.

(9) Xu, Y.; Maddox, P. J.; Couves, J. W. *Chem. Soc. Faraday* **1990**, *86*, 425.

(10) Li, H. Y.; Liang, J.; Liu, Z. M.; Zhao, S. Q.; Wang, R. H. *J. Catal. (China)* **1988**, *9*, 87.

(11) Anderson, M. W.; Sulikowski, B.; Barrie, B. J.; Klinowski, J. *J. Phys. Chem.* **1990**, *94*, 2730.

(12) Wendelbo, R.; Akporiaye, D. E.; Andersen, A.; Dahl, I. M.; Mostad, H. B. *Appl. Catal. A* **1996**, *142*, L197.

(13) Dahl, I. M.; Kolboe, S. *Catal. Lett.* **1993**, *20*, 329.

(14) Dent Glasser, L. S.; Harvey, G. *Proceedings of the 6th International Zeolite Conference*; Olson, D. and Bisio, A., Eds.; Butterworth & Co. Ltd.: Reno, Nevada, 1984; p 925.

(15) Kinrade, S. D.; Swaddle, T. W. *Inorg. Chem.* **1989**, *28*, 1952.

(16) McCormick, A. V.; Bell, A. T.; Radke, C. J. *J. Phys. Chem.* **1989**, *93*, 1741.

(17) Matwiyoff, N. A.; Wageman, W. E. *Inorg. Chem.* **1970**, *9*, 1031.

(18) Sur, S. K.; Bryant, R. G. *Zeolites* **1996**, *16*, 118.

(19) Martinez, E. J.; Girardet, J-.L.; Morat, C. *Inorg. Chem.* **1996**, *35*, 706.

(20) Buslaev, Yu. A.; Petrosyants, S. P. *Koord. Khim.* **1979**, *5*, 163.

(21) Ames, D. P.; Ohashi, S.; Callis, C. F.; van Wazer, J. R. *J. Am. Chem. Soc.* **1959**, *79*, 6350.

(22) Karlik, S. J.; Elgavish, G. A.; Pillai, R. P.; Eichhorn, G. L. *J. Magn. Reson.* **1982**, *49*, 164.

(23) Akitt, J. W.; Greenwood, N. N.; Lester, G. D. *J. Chem. Soc.* **1971**, 2450.

(24) Feng, Q.; Waki, H. *Polyhedron* **1991**, *10*, 659.

(25) Wilson, M. A.; Collin, P. J.; Akitt., J. W. *Anal. Chem.* **1989**, *61*, 1253.

(26) Mortlock, R. F.; Bell, A. T.; Radke, C. J. *J. Phys. Chem.* **1993**, *97*, 767.

(27) Mortlock, R. F.; Bell, A. T.; Radke, C. J. *J. Phys. Chem.* **1993**, *97*, 775.

(28) Miyajima, T.; Maki, H.; Kodama, H.; Ishiguro, S-.I.; Nariai, H.; Motooka, I. *Phosphoreus Res. Bull.* **1996**, *6*, 281.

(29) Miyajima, T.; Kakehashi, R. *Phosphorus Res. Bull.* **1991**, *1*, 101.

(30) Prasad, S.; Chen, W.-H.; Liu, S.-B. *J. Chin. Chem. Soc.* **1992**, *42*, 537.

(31) Prasad, S.; Liu, S.-B. *Microporous Mater.* **1995**, *4*, 391.

(32) Prasad, S.; Liu, S.-B. *Chem. Mater.* **1994**, *6*, 633.

(33) He, H.; Klinowski, J. *J. Phys. Chem.* **1994**, *98*, 1192.

(34) Marcuccilli-Hoffner, F. Etude des milieux de synthese floures de zeolithes et d'aluminophosphates microporeux. Thèse, Université de Haute Alsace, France, 1992.

(35) Shi, J.; Anderson, M. W.; Carr, S. W. *Chem. Mater.* **1996**, *8*, 369.

(36) Led, J. J.; Gesmar, H. *Chem. Rev.* **1991**, 1413.

(37) Harris, R. K. *Nuclear Magnetic Resonance Spectroscopy − a Physicochemical View*; Pitman Books Limited: London, 1983; p 138.

(38) Hansen, E. W.; Vistad, Ø. B.; Akporiaye, D. E.; Lillerud, K. P.; Wendelbo, R. *J. Phys. Chem.*, submitted.

(39) Schaumburg, K.; Deverell, C. *J. Am. Chem. Soc.* **1968**, *90*, 2495.

(40) Stumm, W.; Morgan, J. J. *Aquatic Chemistry − An Introduction Emphasizing Chemical Equilibria in Natural Waters*, 2nd ed.; J. Wiley Sons: New York, 1981; p 241.

(41) O'Reilly, D. E. *J. Phys. Chem.* **1960**, *32*, 1007.

(42) Haraguchi, H.; Fujiwara, S. *J. Phys. Chem.* **1969**, *73*, 3467.

(43) Guth, F. Synthese et caracterisation de solides microporeaux cristallises contenant Al, P et Si. Thèse, Université de Haute Alsace, France, 1989.

(44) Crutchfield, M. M.; Callis, C. F.; Irani, R. R.; Roth, G. C. *Inorg. Chem.* **1962**, *1*, 813.

(45) Loewenstein, W. *Am. Mineral.* **1954**, *39*, 92.

(46) Akitt, J. W.; Elders, J. M. *J. Chem. Soc. Dalton Trans.* **1988**, 1347.

(47) Ren, X.; Komarneni, S.; Roy, D. M. *Zeolites* **1991**, *11*, 142.